A revised hydrological model for the Central Amazon: The importance of emergent canopy trees in the forest water budget

7 authors, including:

Norbert Kunert
Smithsonian Institution
50 PUBLICATIONS **537** CITATIONS

SEE PROFILE

Luiza Maria Teophilo Aparecido
Arizona State University
18 PUBLICATIONS **110** CITATIONS

SEE PROFILE

Niro Higuchi
National Institute for Research in the Amazon - INPA
303 PUBLICATIONS **15,013** CITATIONS

SEE PROFILE

Alessandro Carioca de Araújo
Brazilian Agricultural Research Corporation (EMBRAPA)
110 PUBLICATIONS **2,914** CITATIONS

SEE PROFILE
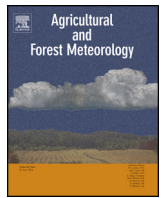
Some of the authors of this publication are also working on these related projects:

Project   Integração Lavoura Pecuária Floresta - ILPF View project

Project   14Constraint View project

A revised hydrological model for the Central Amazon: The importance of emergent canopy trees in the forest water budget

Norbert Kunert [a,b,*], Luiza Maria T. Aparecido [b,1], Stefan Wolff [c], Niro Higuchi [b],
Joaquim dos Santos [b], Alessandro Carioca de Araujo [d], Susan Trumbore [a]

[a] Department of Biogeochemical Processes, Max-Planck-Institute for Biogeochemistry, Jena, Germany
[b] Laboratory of Forest Management, Brazilian National Institute for Research in the Amazon, Manaus, Brazil
[c] Department for Biogeochemistry, Max-Planck Institute for Chemistry, Mainz, Germany
[d] Laboratório de Análises de Sistemas Sustentáveis, Embrapa Amazonia Oriental, Empresa Brasileira de Pesquisa Agropecuária (Embrapa), Belém, Brazil

ARTICLE INFO

ABSTRACT

The Amazon forest is integral to the global climate system in part because of the high rate of rainfall recycling through tree transpiration and biodiversity (size and species composition). However, the partitioning of precipitation into evaporation, transpiration and runoff, has been quantified at only a few sites. At our study site in the central Amazon, annual rainfall in 2013 was 2302 mm and latent heat flux measurements made using eddy covariance revealed that 1360 mm (59%) was returned to the atmosphere through evaporation and transpiration. Runoff accounted for 41% of the net ecosystem water loss. Combining annual xylem sap flux estimates with total stand sap wood area, we estimated annual stand transpiration rate to be 851 mm (36% of annual rainfall). Emergent canopy trees (diameter >30 cm; average height of 28 m) were responsible for the majority (71%) of the transpired water flux, recycling potentially 26% of the rainfall back to the atmosphere. By difference, we estimate that 510 mm of intercepted rainwater (22% of rainfall) was evaporated directly back to atmosphere from the canopy. Highest stand transpiration rates occurred during the dryer months due to both increased water vapor pressure deficit and the onset of new leaf flush. This study provides further evidence for convergent water use characteristics of tropical trees and highlights the importance of large trees in tropical moist forests. Large trees have been demonstrated to be vulnerable to drought-related mortality, and thus potentially will make up a critical component of the response of tropical forests to climate change.

1. Introduction

The Amazon basin represents the largest watershed drained by one primary river and its tributaries (Wohl, 2007), annually discharging about one fifth of the global freshwater supply (Salati and Vose, 1984). Further, the forest ecosystem in the basin is the largest continuous area of tropical forest on our planet and plays an important role in global climatology (Shuttleworth et al., 1984). The Amazon has long been thought to be a self-sustained system with regard to its water and nutrient cycles (Salati and Vose, 1984). The evergreen tropical forest in the central and western Amazon maintains high evapotranspiration rates even during the dry season, as deep-rooting trees can extract soil water from depths below 1 m (Aragao, 2012; Nepstad et al., 1994). Much of the evapotranspired moisture is returned to the forest as rainfall a short distance downwind from its origin (Spracklen et al., 2012) with important cooling effects on the local climate (Kleidon and Heimann, 2000). The forest vegetation also effects precipitation patterns by influencing the abundance and size of cloud condensation nuclei (Spracklen et al., 2012), including direct emissions of dimethyl sulfide (Jardine et al., 2015). Altogether, an estimated 25–56% of the precipitation falling on Amazon forests results from local to regional recycling within the ecosystem (Eltahir and Bras, 1996).

This concept of rainfall recycling by forests was originally described ~35 years ago (Salati and Vose, 1984) based on ecohydrological measurements conducted by Leopoldo et al. (1982). Briefly, the study of Leopoldo et al. (1982) relied on several assumptions. First, the potential evapotranspiration (PET, in mm) in a humid forest is equal to the actual evapotranspiration (ET, in mm) if sufficient

water is available (Villa Nova et al., 1976). Second, the water budget of the forest can be expressed in a simplified equation

$$P = ET + R \qquad (1)$$

where P (mm) is the overall input of water as precipitation, R (mm) is the superficial runoff (assuming only minimal input or loss of water by percolation and baseflow). The water transpired by the forest vegetation (T, in mm) can be estimated indirectly as

$$T = ET - I \qquad (2)$$

where I (mm) is the water intercepted by the forest canopy that is evaporated directly back to the atmosphere. Using this approach, no direct measurement of transpiration by the trees was conducted, and there is no way to assess how the transpiration flux is partitioned among tropical tree functional types that contrast in size, morphology, and ontogeny (Aparecido et al., 2016; Granier et al., 1996b; Horna et al., 2011).

Estimation of the contributions of different tree individuals, each with specific behavior and crown architecture, to the overall transpiration flux in tropical forests is especially difficult because of the high species diversity of tropical forests and the need to sample a representative number of trees to determine average responses (Granier et al., 1996b). The large variation in tree functional traits, including hydraulic structure, could result in considerable variation in the characteristics of diurnal xylem sap flux among individuals (Tyree and Ewers, 1996). However, other studies have shown that species growing together in a common location tend to have converging water use strategies, with strong relationships observed between tree diameter and tree water use rates (Andrade et al., 2005; Jung et al., 2011; Meinzer et al., 2001).

Tree water use rates in closed canopy forests are driven mainly by two regulating parameters, the microclimate above the forest canopy and the soil moisture status (Dierick and Hölscher, 2009; Hinckley et al., 1978). Species-specific responses to these parameters are better observable in monospecific, widely spaced tropical tree plantations (Schwendenmann et al., 2015) than in natural forests. However, tree stands made up of mixed species tend to average out differences among species at the stand level (Kunert et al., 2012). Granier et al. (1996b) described this "smoothed response" of the overall stand transpiration to environmental factors and Meinzer et al. (2001) ascribed it to convergence effects in highly diverse forests. While high tree diversity might create large challenges for upscaling measurements made on individual trees to estimate stand level transpiration, convergent water use strategies would indicate that trees can be classified into broad 'guilds,' defined by their diameter, which is also related to height, canopy position/architecture (Horna et al., 2011), and conductive xylem area (Andrade et al., 2005; Meinzer et al., 2001). Further, if species-specific differences in water use of broadleaved tree species from tropical moist forests can be largely explained by differences in tree diameter, diameter-based water use relationships could be used to estimate stand level transpiration rates (Dierick et al., 2010).

In this study, we used long-term sap flux measurements to test for tree size–water use relationships that can be used for upscaling to the stand level in a species diverse tropical forest. This also allowed us to estimate the relative contribution of trees in different tree size classes (emergent canopy tree, subcanopy trees and understory trees) to the overall stand transpiration rate. We compared the bottom-up transpiration rate to local eddy covariance measurements of evapotranspiration to partition water fluxes into evaporation and transpiration at the stand level. Such partitioning is crucial for understanding processes regulating ecosystem CO_2 exchange and forest productivity (Yepez et al., 2003), and especially for predicting future forest hydrologic feedbacks to climate change and evaluating ecosystem-sustainable harvesting procedures. We compared our results to the hydrological model described by Salati
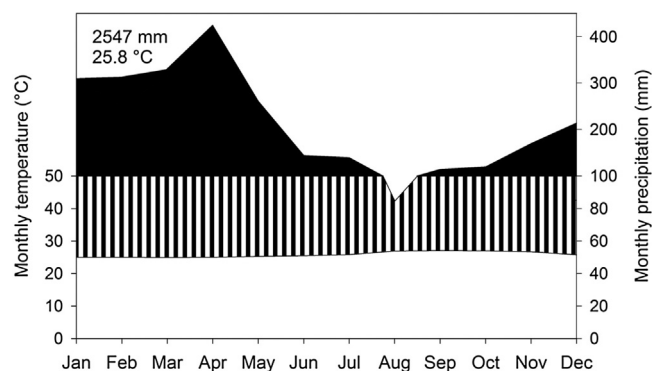

Fig. 1. Climate diagram for the ZF-2 study sites based on data obtained at the LBA-tower at km 34 between January 2000 and December 2012. The LBA-tower is located approximately 14 km away from our study site.

and Vose (1984) in a very similar tropical moist lowland forest (*terra firme*).

2. Material and methods

2.1. Study area

The study was conducted at the Experimental Station for Tropical Silviculture (ZF-2) of the Brazilian National Institute for Amazonian Research (INPA), approximately 60 km northwest of Manaus (02°38′22.54″S 60°09′51.34″W). Average annual rainfall is 2547 mm y^{-1} (Fig. 1). Rainfall is abundant throughout the year reaching its maximum monthly rates in March/April (>300 mm). There is a distinctly dryer season between June and October, though all months except August average more than 100 mm of rainfall per month. In exceptionally dry years monthly rainfall can be below 100 mm between June and October (Kunert et al., 2015b). Air temperature averages 25.8 °C with little variation between seasons (Fig. 1). The study area can be divided in three main vegetation types, mainly determined by the topography (plateaus, slopes and valleys) and soil type. Our measurements, as well as the eddy covariance tower data reported here were made in elevated plateau areas. These plateaus are characterized by well drained clay rich Oxisols and covered with species-rich (>250 species per hectare with diameter >10 cm) evergreen tropical moist forest (*terra firme*) (Chambers et al., 2004). The lower placed valley streams and riverbeds have sand rich Spodosol covered by seasonally inundated tropical moist forest, mainly composed of palm trees (ter Steege et al., 2013). Araújo et al. (2002) estimated that plateau areas on average make up approximately 55% of the area.

2.2. Study sites

Measurements were conducted at three different sites within the ZF-2 area. All tree physiological measurements (Table 1) were conducted in the TACAPE monitoring plots (Tree Assimilation Carbon Allocation Physiology Experiment, S02°36′06.9″ W060°08′05.4″, 115 m a.s.l) located on an approximately 1500 ha plateau area (Jardine et al., 2015). At the TACAPE field site, two one-hectare forest inventory plots were established in the undisturbed old growth forest in 2011 about 18 km on the access road to the field station. The borders of the two inventory plots were about 200 m away from the forest edge to the access road to exclude any edge effects (Kunert et al., 2015b). Trunk base diameter (D_b) was measured of all trees bigger than 10 cm. D_b was measured at 1.3 m or above the buttress (Chambers et al., 2001). Mean basal area of the two inventory plots was 26.2 m^2 ha^{-1}, with an average stem density of 550 tree stems ha^{-1} (Table 2). Mean trunk

Table 1
Summary of species names and characteristics of the 21 study trees.

Species	Family	D_b (cm)	Conductive xylem area (cm^2)	Crown projection (m^2)	Height (m)	Canopy class
Neea sp.	Nyctaginaceae	11.5	63.7	7	12	Understory
Protium paniculatum Engl.	Burseraceae	12.5	73.8	4	14	Understory
Myrcia paivae O.Berg	Myrtaceae	13	79.2	6	15	Understory
Agonandra brasiliensis Miers ex Benth. & Hook.f.	Opiliaceae	13	79.2	7	11	Understory
Aspidosperma vargasii A.DC.	Apocynaceae	15.5	108.3	18	17	Understory
Myrcia subsericea A.Gray	Myrtaceae	15.5	108.3	28	14	Understory
Clarisia racemosa Ruiz & Pav.	Moraceae	16	114.6	23	18	Understory
Unknown	Lecythidaceae	17	127.7	17	17	Understory
Virola sp	Myristicaceae	18.6	149.8	30	23	Understory
Sloanea sp.	Elaeocarpaceae	19	155.6	52	20	Understory
Pouteria erythrochrysa T.D.Penn.	Sapotaceae	20.0	166.0	57	26	Subcanopy
Pouteria retinervis T.D.Penn.	Sapotaceae	21.3	190.7	37	25	Subcanopy
Rinorea guianensis Aubl.	Violaceae	25	253.7	86	21	Subcanopy
Erisma bicolor Ducke	Vochysiaceae	26	272.0	101	22	Subcanopy
Protium paniculatum Engl.	Burseraceae	26	272.0	126	25	Subcanopy
Licaria crassifolia (Pior.) P.L.R. Morales	Lauraceae	26.5	281.4	75	26	Subcanopy
Virola calophylla (Spruce) Warb.	Myristicaceae	37	509.8	185	27	Emergent
Protium altsonii Sandwith	Burseraceae	43.5	680.1	198	27	Emergent
Corythophora alta R.Knuth	Lecythidacea	44	694.1	259	28	Emergent
Plethogyne catingae Duke	Fabaceae	48.5	825.5	242	26	Emergent
Maquira sclerophylla (Ducke) C.C.Berg	Moraceae	54	999.5	270	28	Emergent

Table 2
Summary of the plot characteristics of the two 1 ha inventory plots.

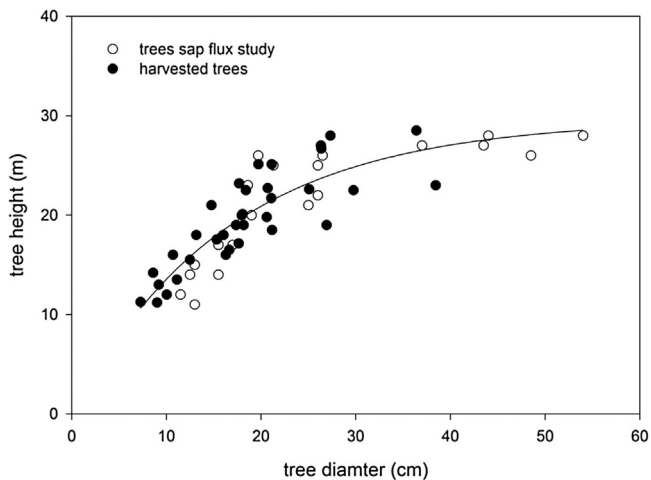| Size class	D_b range (cm)	Stems ha^{-1}	Size range distribution (%)	BA (m^2 ha^{-1})	SA (m^2 ha^{-1})
Understory	10–19.9	347	63	5.6	3.2
Subcanopy	20–29.9	114	21	5.5	2.8
Emergent	>30	89	16	15.2	6.8
Total		549	100	26.2	12.9

Fig. 2. Relationship between trunk base diamter (D_b) and tree height for the 34 harvested trees (solid circles, height was measured after cuttung the tree) and the 21 trees of the sap flux study (open circles, height was estimates with a Biltmore stick). The fitted exponential model was: ($y = 29.6249 \cdot 1 - exp^{(-0.0611 \cdot x)}$), with y being "tree height" and x as "tree diameter"; $R^2_{adj} = 0.76$, P < 0.0001).

base diameter was 21 ± 12 cm. Average canopy height was around 28.4 m (compare Fig. 2), measured through destructive sampling (harvesting) about 250 m away from the TACAPE monitoring plots, close to the access road. The other site was at the K34 tower of the LBA-experiment (Large Scale Biosphere-Atmosphere Experiment), which is located approximately 8 km away of the TACAPE-area on a medium sized plateau (2°36″32.67′ S, 60°12″33.48′ W, 130 m asl). The aluminum-structured tower with a base area of 1.5 m × 2.5 m and a height of 50 m was erected in 1999 (Araújo et al., 2002). The TACAPE area is within the outer footprint of the eddy covariance tower measurements (Araújo et al., 2002).

2.3. Meteorological measurements

Climate data was available from three different sites in the study area. Climate data from the K34 LBA eddy flux tower are available since January 2000, and described in more detail below (for more details sensor set up see Araújo et al., 2002). In addition to the climate station at the K34 LBA-tower, we recorded air temperature (°C), relative humidity (%) and precipitation (mm) at half-hourly intervals at 2.2 m above the ground with a weather station consisting out of a thermohygrometer, an anemometer, a barometer and a rainbucket (PCE-FWS 20, PCE Inst., Meschede, Germany) in open terrain adjacent to the field camp of the Experimental Station for Tropical Silviculture (ZF-2), approximately 4 km away from the TACAPE field site in the direction to the K34 tower. In addition, a Quantum Sensor (LI-190A, Licor Inc., Lincoln, USA) was set up at the same height as the weather station to record Photosynthetic Photon Flux Density (PPFD, $\mu mol \, s^{-1} \, m^{-2}$). One additional climate station was installed at the road margin next to the TACAPE – study site. To assess the climatic conditions within the forest, we set up an automatic thermohygrometer (Voltcraft DL121TH, Conrad Electronic Ltd., Barking, UK) to record air temperature and humidity at half-hourly intervals at 2.2 m. We tested the accuracy of the thermohygrometer by measuring humidity and temperature for several days next to the weather station at the ZF-2 camp site. The variation between the two instruments was lower than the accuracy of the instruments given by the manufacturer (T ± 1 °C and RH ± 3%).

2.4. Eddy covariance data

We used eddy covariance (EC) data collected from the ZF2-K34 tower from 1 of January 2013–31 of December 2013 to estimate the evapotranspiration rate. The eddy-covariance system consists of a triaxial sonic anemometer (CSAT3, Campbell Scientific, Logan, UT, USA) and an open-path infrared gas analyzer (IRGA, LI-7500, Li-Cor,

Lincoln, NE, USA) was used to measure latent heat flux (LE), vertical wind velocity, scalar concentrations of water vapor and CO_2 at a frequency of 10 Hz. Filtered flow statistics were recorded in real time half-hourly averages by a CR23X data logger (Campbell Scientific) (Katul et al., 1997). More details on sensor set up and data processing are given in Araújo et al. (2002). The raw data were processed using the correction methods of the Alteddy software (version 3.6 until August 2013 and version 3.9 since September 2013; www.climatexchange.nl/projects/alteddy/). A 2D rotation axis type was used and the correction angle of attack was processed following the procedure of Nakai and Shimoyama (2012). No gap filling was applied. Data were made available on request by the LBA Project office of the Brazilian Ministry of Science and Technology at INPA in Manaus, Brazil.

2.5. Xylem sap flux measurements

A data logger was placed (CR10x; AM16/32a multiplexer, Campbell Scientific Inc., Logan, UT, USA) in one of the TACAPE – inventory plots. A subsection of the TACAPE – plot was chosen with a minimum of natural forest disturbance, such as tree fall gaps or standing dead trees and with a representative tree size class distribution of an old growth forest (i.e. with comparable size class distribution for the TACAPE inventory plots (Table 2) and the trees equipped with sensors (Table 3)). All trees with $D_b > 10$ cm within a 12.6 m radius of the data logger (approximately 500 m^2 of ground area, or 5% of the area of a one hectare inventory plot) were equipped with xylem sap flux sensors. In total 21 trees from three different tree size classes (5 emergent canopy trees ($D_b > 30$ cm), 6 subcanopy trees ($D_b = 20$–30 cm) and 10 understory trees ($D_b = 10$–20 cm)) were equipped with xylem sap flux sensors (Table 1; details on the definition of tree size classes in section: *Tree characteristics, stand structure and leaf area*).

A set of two Granier type (heat dissipation method) xylem sap flux sensors were installed at breast height (1.30 m) in each sample tree (Granier, 1985). The sensors were installed in differing cardinal directions of the stem to exclude eventual heating effects of direct sunlight on the tree stems and to assess tree internal difference in xylem sap flux velocities. Each of the Granier thermal dissipation sensors consisted of a heated and a reference probe, each 2 cm long. Both probes were inserted into heat distributing aluminum tubes (Granier, 1985). The tips of the tubes were sealed with epoxy to prevent fast degradation, including dissolution of the probes by exudates commonly found in tropical trees. The heated probe was placed approximately 12–15 cm above the reference probe (Granier, 1987). We shielded the sensors with small aluminum-coated boxes to protect the sensors from external thermal influence and covered them with plastic foil for rain protection. Over the entire study period all heated probes were constantly supplied with 0.2 W power. The data logger read the voltage output from the thermocouples every 30 s and stored 15 min averages. The voltage output was used to calculate xylem sap flux density (J_s, g cm^{-2} h^{-1}) with the standard Granier equation (Granier, 1987):

$$J_s = 3600 \times 0.0119 \times \left[\frac{\Delta V - \Delta V_{ref}}{\Delta V} \right]^{1.231} \qquad (3)$$

where ΔV (mV) is the measured voltage difference between the two probes and ΔV_{ref} the reference voltage difference measured at a time of zero flow (at night). In the rare cases where sensors failed (i.e. if null, out of range, erratic or negative readings were obtained) we inserted a new sensor into the xylem a few centimeters to the right or left of the old sensor, using newly drilled holes to avoid sampling errors due to tissue injury or xylem embolism (Ford et al., 2007; Moore et al., 2010). When data was missing, gap filling was performed as suggested in Kunert (2016). Briefly, sap

flux densities for missing days were modeled based on the size class-specific relationships between measured sap flux densities and PPFD ($r^2 = 0.67$–0.89, p < 0.05).

2.6. Estimation of the conductive xylem

In a first attempt, we applied a commonly used method to estimate the conductive xylem area (A_x, m^2). We injected an indigo carmine solution into the tree stems and extracted stem cores about 10 cm above the injection point after 2 h (compare Andrade et al., 2005; Meinzer et al., 1999, 2001). However, the solution did not appear in the cores even after waiting a longer time period, perhaps reflecting very slow vertical velocities of xylem sap in the Central Amazon compared to other forests (Dünisch and Morais, 2002; Kunert et al., 2013, 2012 Kunert and Mercado Cardenas, 2012). Further, we wanted to assure that we assessed the entire sapwood area and the injection reached the heartwood, which was not reliable with this method. In a second attempt, we used a destructive method to determine A_x. We selected 34 trees in a plot with easy access to the road, but at least 400 m away from the plot where xylem sap flux measurements were conducted to avoid edge effects (Kunert et al., 2015b). The diameter of the selected tree individuals varied between 5 and 40 cm. We limited the diameter up to 40 cm, considering the limitations of transportation, laboratory analyses and handling. Trees were then harvested between December 2012 and May 2013, when weather conditions were representative for most of the other months of the year (Van de Wal et al., 2015). After harvesting, stem segments of 30–40 cm length were cut out of the trees at breast height and immediately placed upright in a bucket holding a solution of indigo carmine. Blue stains appeared usually within two to three hours on the upper surface the stem segments. The area of colored cross section was assumed to represent the conductive xylem. Conductive xylem area was measured using five radii marked along the cross-section starting from the pith. The first radius was equivalent to the largest radius; the second was marked 45° from the first; and the other three were 90° from each other. The 34 harvested trees belonged to 27 different species, but we had some overlap with the species pool of trees chosen for the sap flux study. An allometric relationship was established between measured conductive area and D_b (Fig. 3). The conductive sap wood area of a given tree could thus be estimated as:

$$A_x = 0.8227 \times D_b^{1.7805}; (R_{adj}^2 = 0.47, p < 0.0001) \qquad (4)$$

The curve agrees with other relationships made with larger trees reported in the literature (Fig. 3) (Anhuf et al., 1999; Aparecido et al., 2016; Granier et al., 1996a; Horna et al., 2011; Motzer et al., 2005; Parolin et al., 2008). We therefore used it to extrapolate sapwood area for trees with $D_b > 50$ cm for which we have no independent measure of sapwood area. The conductive sap wood area for one hectare of forests (A_{plot}, m^2) or one tree size class (A_{size}, m^2) was calculated as the sum of A_x of all trees in a hectare or given tree size class. We averaged the total of the stem numbers of our two 1 ha plots for the uspcaling (Table 2). We estimated stand transpiration (T_{stand}, mm d^{-1}) for certain time intervals (days, months and one year) and tree size classes (emergent tree, subcanopy tree, understory tree). Therefore, the respective J_s of a given time period (daily, monthly and annually) or tree size class was multiplied by A_{plot} or A_{size} and divided by the total plot area (Granier et al., 2000). Individual tree water use (Q, kg d^{-1}) was calculated for the sample trees with sensors installed by multiplying the daily xylem sap flux rate (J_s, g cm^2 d^{-1}) of a given tree with its conductive sapwood area (A_{tree}, cm^2).

Table 3

Summary of water use characteristics of the different tree size classes. Mean values with standard deviations are given for the maximum xylem sap flux density (J_{smax}, g cm^{-2} h^{-1}), maximum daily sap flux density (J_s, g m^{-2} h^{-1}) and maximum daily tree water use rate (Q, kg d^{-1}). The values for maximum daily sap flux density and maximum daily tree water use rate are also given for differenced seasons. Lower-case letters indicate significant differences ($p < 0.05$) for a given tree size class between. dry and wet season (paired Student's t-test). Capital letters indicate significant differences among size classes in a given season daily J_s: ANOVA followed by a Brown-Forsythe test; daily Q: ANCOVA with D_b as covariate followed by a post hoc Tukey HSD test.

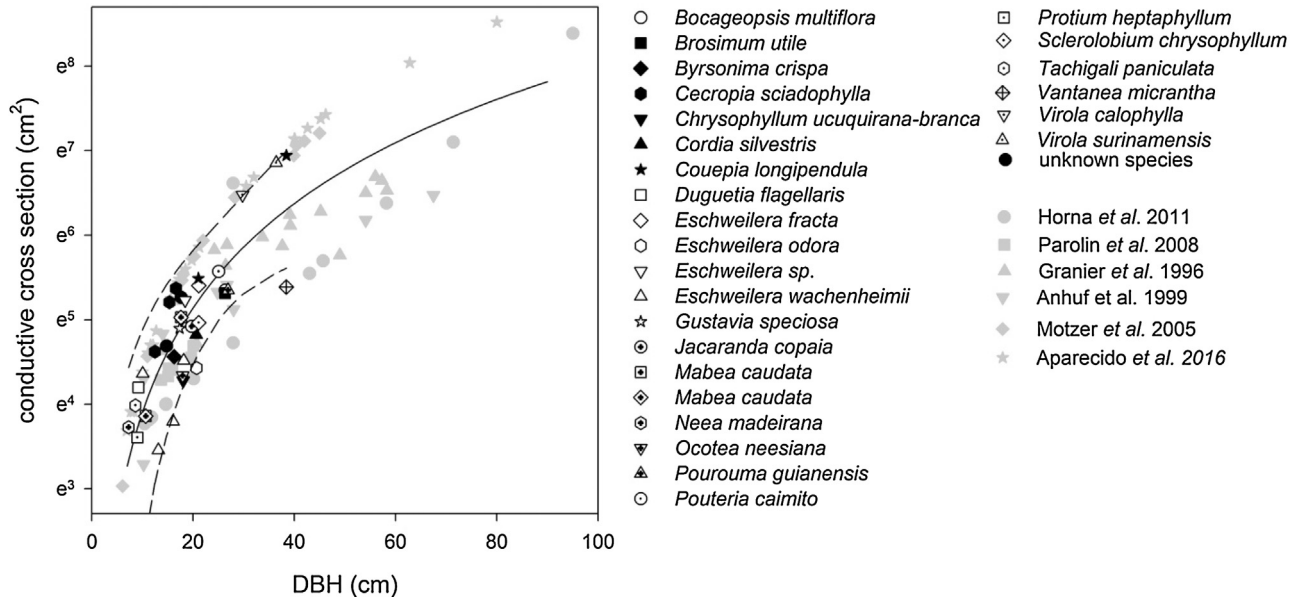| Size class	Sample size	Size range distribution (%)	J_{smax} (g cm^{-2} h^{-1})		Daily J_s				Daily Q			
					wet (g cm^{-2} d^{-1})		dry (g cm^{-2} d^{-1})		wet (kg d^{-1})		dry (kg d^{-1})	
			Mean	SD	Mean	SD	Mean	SD	Mean	SD	Mean	SD
Understory	10	48	7	2.5	44.4[a,A]	14.2	52.6[a,A]	18.9	3.8[a,A]	1.2	4.5[a,A]	1.6
Subcanopy	6	29	10.2	2.2	69.4[a,B]	14.9	76.1[a,B]	16.4	16.7[a,A]	4.8	18.3[a,A]	5.3
Emergent	5	24	10.3	4.1	68.6[a,B]	25.2	77.1[a,B]	30.6	178.9[a,A]	60.5	201.2[b,A]	73.4

Fig. 3. Conductive cross-section as a function of trunk base diameter (D_b). The fitted curve includes only data from this study. ($A_x = 0.8227 \cdot D_b^{1.7805}$; $R^2_{adj} = 0.47$, $p < 0.0001$). The short dashed lines represent the 95% Confidence Interval for the fitted curve based on our data set. Literature values are highlighted in grey assorted symbols (Anhuf et al., 1999; Aparecido et al., 2016; Granier et al., 1996b; Horna et al., 2011; Motzer et al., 2005; Parolin et al., 2008).

2.7. Tree characteristics, stand structure and leaf area

We used a Biltmore stick to estimate the heights of the standing trees equipped with xylem sap flux sensors (Anon, 1998). Other characteristics of the studied trees are given in Table 1. There is a very strong relationship between tree height and tree diameter in the area (Higuchi et al., 1998). We used this relationship to define which trees were emergent canopy trees, sub canopy trees and understory trees (Fig. 2). Trees >30 cm D_b achieved the local average forest canopy height of 28 m, and were classified as emergent canopy trees. We assigned trees between 20 and 30 cm D_b as subcanopy trees, and those between 10 and 20 cm D_b as understory trees. Subcanopy trees could reach the maximum height of 28 m, but were at least partly shaded by emergent trees. The maximum height of the suppressed understory trees was 23 m and trees in this class were always completely shaded by taller neighboring trees. The canopy position of a given tree was further assessed visually to make sure that all individuals fit the size class definition by tree height and diameter.

To assess changes in leaf cover over the study period, we took hemispherical photographs in six fixed locations underneath the sampled trees to obtain leaf area index (LAI, m^2 m^{-2}). We used a digital camera (Minolta Dimage Xt, Chuo-Ku, Osaka, Japan) equipped with a 185-fish-eye lens and a leveling device (Regent Instruments, Sainte-Foy, Quebec, Canada). Pictures were taken

monthly or more frequently if we observed major changes in tree phenology. Leaf area and canopy openness were calculated by analyzing the hemispherical pictures with Gap Light Analyzer Version 2.0 (GLA, Simon Fraser University, Burnaby, BC, Canada).

2.8. Data analyses

We defined a dry season when less than 100 mm month^{-1} of rainfall was measured (Dietrich et al., 1996). Accordingly, the dry season in the year 2013 lasted from June until September (July had 117.9 mm of rainfall due to a single heavy rain event). The periods from January until May and October until December were defined as wet season (compare Kunert et al., 2015b). We performed a Monte Carlo simulation to estimate the uncertainty of A_{plot} using the standard error of the coefficients of the sapwood allometric equation (Eq. (4)) and assumed a normal distribution about their averages. Random individual trees were sampled from the distribution and the conductive sapwood area for each tree in the inventory plots was calculated 1000 times. We used the standard deviation of the distribution of the averages (i.e. the standard error of the mean) as an estimate of the uncertainty of A_{plot} and for a given size class (A_{size}). Maximum xylem sap flux density was defined at the daily maximum value that persists for at least 45 min with a maximum variation of 5%. The maximum tree water use (Q_{max}) was defined as the absolute daily maximum found over the entire

study period. Differences in xylem sap flux densities and tree water use rates between different seasons were determined with a paired Student's t-test. An analysis of variance (One-way ANOVA followed by a Brown-Forsythe test) was performed to test for homogeneity of xylem sap flux densities between different size classes. Tree water use rates among tree size classes were compared using the analysis of covariance with D_b as a covariate (ANCOVA, followed by a post hoc Tukey HSD test). Linear and nonlinear regressions were applied to assess the relationship (coefficient of determination and probability – R^2 and p-value, respectively) between water use characterists (Q_{max} and T_{stand}) and the explaining variables tree size and meteorological data. Statistical analyses were performed with SPSS 16.0 (SPSS Inc., Chicago, USA).

3. Results

3.1. Meteorological measurements

Precipitation varied among the three sites where it was measured. During the 12-month study period a total of 2302 mm was measured at the ZF2-camp site climate station. The annual precipitation recorded at the forest margin at the TACAPE-site was 2167 mm. Unfortunately, the annual sum of precipitation was not available from the K34 LBA-tower due to a sensor failure that lasted several weeks. However, comparing the months with existing data sets between 2011 and 2013, the K34 station received on average 7 and 11% more rain than the ZF-2 campsite and the TACAPE-field site, respectively. This indicates a distinct rainfall gradient along the ZF-2 road from the BR-174 toward the Cuieiras River. Measured values of PPFD and VPD differed between the wet months and the dryer months at all climate stations. For example (values represent mean values ± SD), PPFD averaged $31.4 \pm 6.9 \, \text{mol} \, \text{m}^{-2} \text{day}^{-1}$ and VPD averaged $0.21 \pm 0.14 \, \text{kPa}$ during the wet months at the climate station at the forest margin of the TACAPE field site and, respectively, $38.0 \pm 8.6 \, \text{m}^{-2} \text{day}^{-1}$ and $0.65 \pm 0.19 \, \text{kPa}$ during the dryer months.

3.2. Leaf phenology

Mean leaf area index was $5.09 \pm 0.54 \, \text{m}^2 \, \text{m}^{-2}$ with a canopy closure of 98% in the study plot. There was no significant difference between the leaf area index in the dry season and the wet season. Leaf area dropped only to $4.93 \pm 0.53 \, \text{m}^2 \, \text{m}^{-2}$ at the peak of the dry season (end of August) compared to the peak of the wet season with $5.40 \pm 0.46 \, \text{m}^2 \, \text{m}^{-2}$ in May. There were two notable leaf shedding events with an increased leaf litter accumulation at the forest floor. The first leaf shedding event occurred at the onset of the dryer period in June. Most of the trees in the study plot, where a change in leaf cover was notable, were flushing new leaves while the old leaves were still attached to the branches. The second leaf shedding event was after the first heavy rainfalls with over 30 mm of rain in a 24 h period in mid-October. Leaf area dropped to $3.51 \pm 0.16 \, \text{m}^2 \, \text{m}^{-2}$, but increased again to almost $5 \, \text{m}^2 \, \text{m}^{-2}$ within 7–10 days.

3.3. Variation in xylem sap flux and water use rates of the sample trees

Maximum xylem sap flux density was highest in the emergent canopy tree *Corythophora alta* ($15.1 \, \text{g} \, \text{cm}^{-2} \, \text{h}^{-1}$, 44 cm in diameter) and smallest in an understory tree *Clarisia racemosa* ($3.0 \, \text{g} \, \text{cm}^{-2} \, \text{h}^{-1}$, 16 cm in diameter). Mean maximum sap flux density for emergent canopy trees was $6.8 \pm 4.2 \, \text{g} \, \text{cm}^{-2} \, \text{h}^{-1}$ during wet and rainy months and $9.9 \pm 38 \, \text{g} \, \text{cm}^{-2} \, \text{h}^{-1}$ during dry months with high evaporative demand (Table 3). The subcanopy trees reached maximum xylem sap flux densities of $8.9 \pm 1.8 \, \text{g} \, \text{cm}^{-2} \, \text{h}^{-1}$ during wet
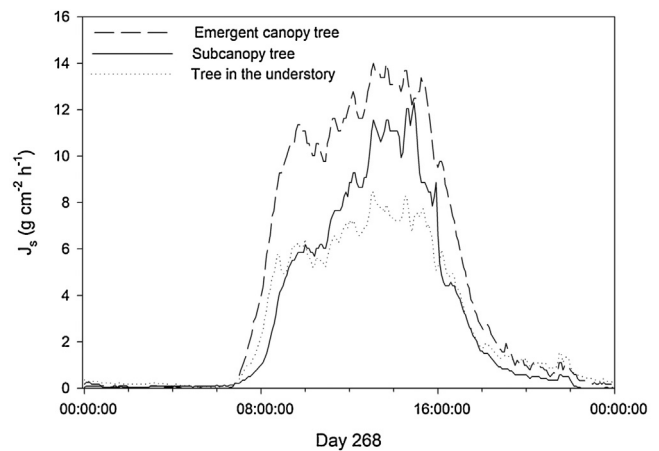

Fig. 4. Diurnal course of the xylem sap flux density (Js) of a representative emergent canopy tree, a subcanopy tree and a understory tree. Note: The emergent tree has a fully sun exposed crown; xylem sap flux density is high starting early morning and remains high until late afternoon. The subcanopy tree is shaded by another tree during the morning hours, but is receiving full sun light after 12 PM. Xylem sap flux densities of the subcanopy tree are low in the morning and high during the afternoon. The understory tree is shaded by another tree for the entire day, resulting in a xylem sap flux denstiy lower than the other categories.

months and $10.2 \pm 2.2 \, \text{g} \, \text{cm}^{-2} \, \text{h}^{-1}$ during dry months. Average maximum xylem sap flux densities found in understory trees was $7.0 \pm 2.5 \, \text{g} \, \text{cm}^{-2} \, \text{h}^{-1}$ during wet months and $7.2 \pm 2.8 \, \text{g} \, \text{cm}^{-2} \, \text{h}^{-1}$ during dry months. Mean daily sap flux densities were significantly higher ($p < 0.05$) for the emergent canopy and subcanopy trees than the understory trees (Table 3).

The three size classes followed distinct patterns of diurnal course of sap flux density (Fig. 4). Emergent trees had a typical bell shaped xylem sap flux curve on bright sunny days. Subcanopy trees that were partly shaded, were characterized by a peak in xylem sap flux when their crowns or fractions of the crowns were exposed directly to the sun. The xylem sap flux curves of understory trees followed a bell-shaped curve with maximum values at local noon, but reached much lower maximum values than emergent canopy trees (Table 3).

We found a wide range of mean annual water use rates. Maximum water use was strongly correlated with the D_b of the trees (Fig. 5, $R^2_{adj} = 0.91$, P < 0.0001). Minimum values ranged from $0.19 \, \text{kg} \, \text{day}^{-1}$ measured in understory trees to maximum values of $189.1 \, \text{kg} \, \text{day}^{-1}$ recorded for an emergent canopy tree (*Plethogyne catingae*, 48.5 cm in diameter). Rates of water use for most of the canopy trees were highest during the dryer months. In contrast, no statistically significant effects of season were observed for the understory trees (Table 3).

3.4. Sapwood area and stand transpiration separated into size classes

The total sapwood area of all trees bigger than 10 cm in D_b in our two inventory plots averaged $12.9 \, \text{m}^2$ of conductive xylem per hectare, indicating that 49% of the stand's basal area (26.2m^2) was conductive. On average, per one hectare of forest, 89 trees had $D_b > 30$ cm, i.e. were classified as emergent canopy trees. These contributed $6.8 \, \text{m}^2$ or 53% of the conductive sapwood area of the forest stand. Consequently, 114 subcanopy trees (D_b: 20–30 cm) made up 22% of the conductive area of the stand, and 347 understory trees (D_b: 10–20 cm) 25% of conductive sap wood area of the stand. Interestingly, the (on average) six trees per plot with $D_b > 70$ cm contributed 10% of the conductive sapwood area and stored 11% of the living biomass of the plot (allometric equation for biomass estimation: $\ln(\text{biomass}) = -0.37 + 0.333 \ln(D_b) + 0.933$
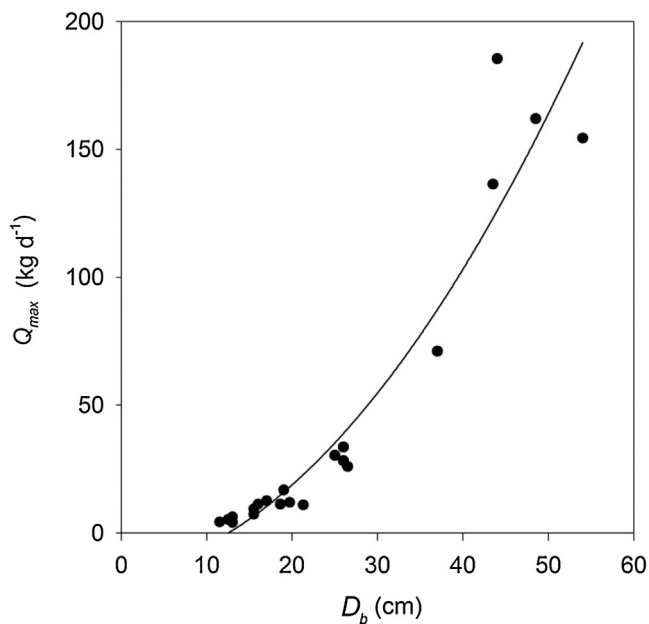
Fig. 5. Maximum tree water use (Q_{max}, kg d^{-1}) in relation to trunk base diameter (D_b, cm) (R^2_{adj} = 0.91, P < 0.0001).

$\ln(D_b)^2 - 0.122 \ln(D_b)^3$; Chambers et al., 2001). Stand transpiration rates were dominated by contributions from the emergent canopy trees, which contributed 71% or 602 mm a^{-1} of the annual stand transpiration rate of 851 mm a^{-1}, while subcanopy trees transpired another 148 mm a^{-1} (17%), and understory trees only contributed 101 mm a^{-1} (12% of annual stand transpiration).

3.5. Partitioning of the water budget

Annual precipitation recorded at our climate station at the ZF-2 camp site reached 2302 mm in 2013. February, with 430 mm of rainfall, was as the wettest month of the year while September with only 47 mm was the driest month. The annual evapotranspiration measured by the eddy covariance system was 1360 mm, with higher monthly evapotranspiration rates during the dry season than during the wet season. Monthly values of evapotranspiration estimated from the eddy covariance system ranged between 83 mm and 153 mm, corresponding to the values of the wettest and driest month, respectively (Fig. 6). Assuming the same rainfall at our sapflux measurement site, emergent canopy trees transpired 37% of the annual rainfall, subcanopy Trees 6%, and understory Trees 4% (Fig. 8). Canopy transpiration increased throughout the dryer months from July until October and reached its monthly maximum in October with 141 mm (Fig. 6). Maximum transpiration during the dry season was, thus, five times higher than in the wettest months (February to May) of the year when a monthly transpiration rate of on average of only 37 mm. Daily stand transpiration was related to PPFD above the canopy (Fig. 7), though slopes were steeper in dryer months (July, August and September) compared to the wettest months (January, February and March).

4. Discussion

4.1. Emergent canopy trees dominate transpiration in tropical moist forests

Our results show that emergent canopy trees are an essential component in the hydrological cycle in tropical old growth forests. Trees over 30 cm in diameter recycled most of the water

(71% of stand transpiration), and were responsible for most of the aboveground biomass, within the Central Amazon tropical forest we studied. Globally, the number of big trees in tropical forests is declining, due to a combination of deforestation, logging and natural disturbance events (Lindenmayer et al., 2012). Together, emergent and subcanopy trees, which were only a third of the individuals in the plot, were responsible for 88% of the entire stand transpiration. A study in Indonesia found even more extreme results, that canopy trees were responsible for 90% of the annual transpiration (Horna et al., 2011); and a very recent study in Costa Rica found similar results, in which dominant trees were on average responsible for 76% of the stand transpiration (Aparecido et al., 2016). Emergent trees also made up 57% of the basal area in our plots and make up a large proportion of the biomass and carbon storage in most Amazonian tropical forests (Brown et al., 1995; Slik et al., 2013). As noted by Vieira et al. (2004), the forests in the Manaus region have biomass more evenly distributed among size classes than other forests with more pronounced dry seasons, so this effect may be even greater at other sites in the Amazon.

4.2. Why do emergent canopy trees use more water?

The humid tropics are systems with high humidity that have high cloud coverage over several months per year (Ghazoul and Sheil, 2010). Hence, low evaporative demand of the atmosphere and low boundary layer conductance can limit transpiration (Kunert et al., 2015b; Meinzer et al., 1997). Low xylem sap flux in the understory can further be explained by phase diffusion limitation due to leaf wetness (Aparecido et al., 2016; Meinzer et al., 2004; O'Brien et al., 2004; Schneebeli et al., 2011). Leaf wetting in the forest canopy is a frequent event at our study site and can generally limit understory transpiration, since little solar radiation reaches the understory canopy and therefore wet leaves dry more slowly than in other canopy levels (Aparecido et al., 2016; Motzer et al., 2005). Further, the relatively high air humidity in the forest understory and, thus, the low vapor pressure deficit, reduces the xylem sap flux, especially at our study site (Kunert et al., 2015b). Subcanopy and understory trees are usually completely or partly shaded by other trees what reduces their sap flux rates (Fig. 4). In contrast, the emergent canopy trees are exposed to air that mixes with dryer air in the planetary boundary layer and therefore has higher vapor pressure deficit than lower levels of the forest canopy (Kunert et al., 2015b). Tall trees, thus, are able to release more water through the stomata (Giambelluca et al., 2003). This 'clothes-line' effect helps trees release water vapor into the almost water vapor saturated atmosphere (Ghazoul and Sheil, 2010).

Higher transpiration rates can be maintained during dry seasons via water uptake by deep root systems. These play a considerable role at the stand level by redistributing deep soil water during months with water input deficit (da Rocha et al., 2004; Nepstad et al., 1994). Trees also store water in their trunks, and this is thought to contribute ~10% of the transpired water for all three tree size classes (Meinzer et al., 2004). These hydraulic limitations and the delayed response time of the xylem sap flux system raise the question whether emergent canopy trees are more susceptible to drought stress during exceptionally dry years (Kunert, 2016). For example during the drought years in 2005 and 2010, especially the large canopy tree showed subsequent elevated mortality rates (Brienen et al., 2015).

4.3. Revised water budget

The central Amazonian forest stand we studied transpires 37% (or 851 mm) of the annual water input via rainfall back to the atmosphere. The first water budget drawn by Salati and Vose (1984), working at the Adolfo Ducke Forest Reserve about 50 km from our
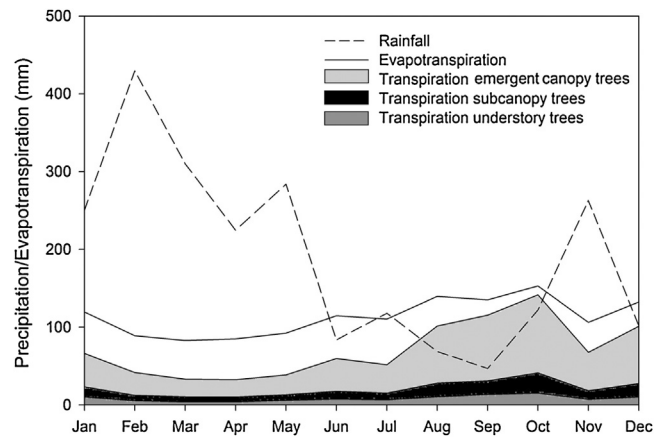
Fig. 6. Annual course of rainfall, evapotranspiration and stand transpiration. The quantity of each tree-size transpiration is represented by the thickness of the bar. All tree transpiration bars are adding up to the overall stand transpiration. Note: There was higher output via evapotranspiration than input by precipitation in June, August and Spetember.
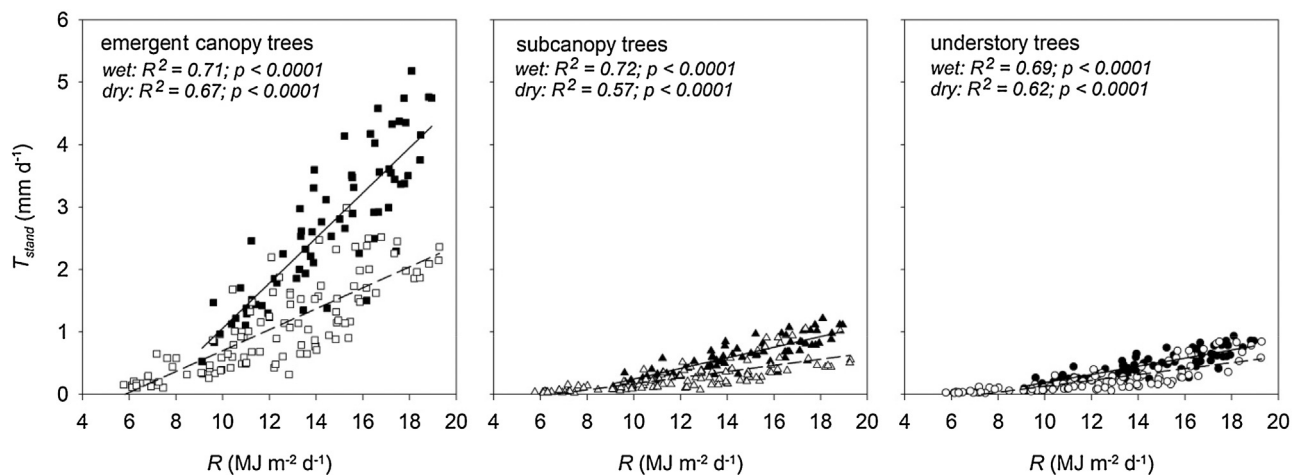

Fig. 7. Linear relationships between global radiation (R; MJ m^{-2} d^{-1}) and daily stand transpiration rate (T; mm d^{-1}) separated into different size classes during wet months (empty symbols) and dry months (solid symbols).

site, estimated that approximately 50% (or approximately 960 mm) of the rainfall is recycled through tree transpiration. Salati and Vose (1984) measured an average annual rainfall of 2000 mm during their two-year study period, significantly less rain compared to the 2302 mm in our study in the 2013. Considering the variation in annual rainfall between the study by Salati and Vose (1984) and our study, the percentage of rainfall recycling might differ, but the actual transpiration rates are very similar. Nevertheless, the transpiration estimates can vary largely from year to year and in different ecosystems. The few existing studies that present annual transpiration rates are based throughout on sap flux measurement of limited duration between a couple of months and one and a half years in the maximum (compare Aparecido et al., 2016; Horna et al., 2011; Kunert et al., 2015a). The reported annual stand transpiration rates and their contribution to the recycling rate are highly variable, reflecting the diversity of ecosystems and especially reflecting the variation in precipitation. For example trees transpired only 9% (253 mm) of the annual precipitation (∼3500 mm a year) in a perhumid tropical premontane forest in Asia (Horna et al., 2011) and approximately 11% (497 mm) in a moist Costa Rican cloud forest with about 4500 mm of precipitation a year (Aparecido et al., 2016). The Amazonian moist tropical lowland forest we studied has lower annual precipitation and much higher annual stand transpiration rates that significantly increase with forest disturbance, suggesting that transpiration rates reflect driving forces (sunlight

and atmospheric mixing that reduces relative humidity) rather than fluctuations in water supply from the soil. Accordingly, 37% (845 mm) of the annual rainfall is recycled in undisturbed stands and up to 57% (1320 mm) in highly disturbed forests (Kunert et al., 2015b). The moist gradient shows the limitations of studies based on only one year of measurements, if interannual variation in rainfall pattern is high. In areas with a large interannual rainfall variation, long-term studies assessing tree water fluxes might be necessary to give a better representation of the actual water balance. Nevertheless, our data provides strong supporting evidence of a high recycling rate of precipitation by trees and the view of the Amazon as a self-sustaining system (Salati and Vose, 1984). Our study suggests that forest cover in the Amazon Basin plays an important role in the current precipitation pattern over large parts of the South American subcontinent (Spracklen et al., 2012).

We also documented the function of trees as "water pumps" (Aragao, 2012), extracting water from the soil to maintain or increase transpiration rates during the dryer months of the year. During the wet season, trees transpired less than 40% of ET (evapotranspiration), while in a dry season month (August), tree transpiration made up almost 95% of ET. LAI did not change with seasons significantly, but the enhanced transpiration rate in the dryer months accompanies leaf flush and increased photosynthetic rates observed in the Amazon during the dry season (Morton et al., 2014). At the same time, higher vapor pressure deficit in the dry
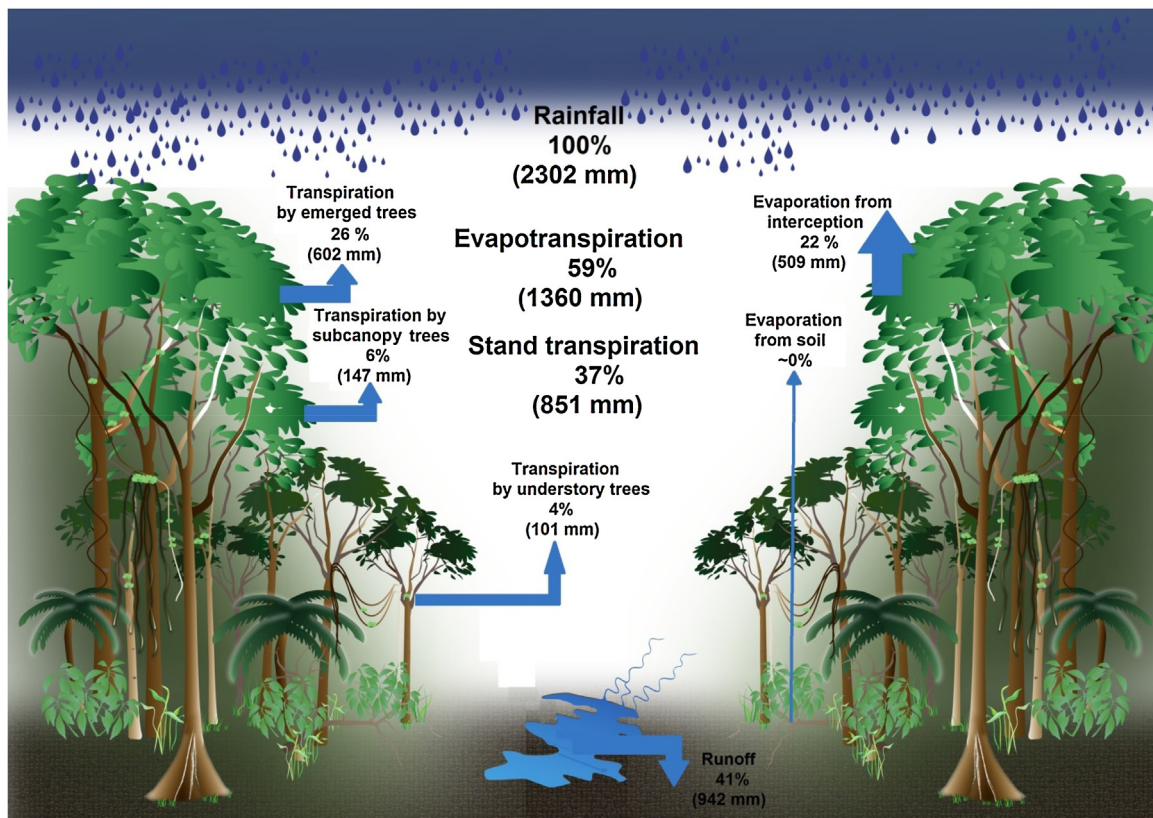
Fig. 8. Water balance of the *terra firme* forest of the present study in 2013.

season, especially dryer stand climate in the forest interior (Kunert et al., 2015b) enhances tree transpiration, rather than the higher solar irradiance as often stated in the literature (Aparecido et al., 2016; Huete et al., 2006; Saleska et al., 2003 Wright and Schaik, 1994). However, the enhancement of transpiration – i.e. continual water supply – has important implications on stomatal gas exchange and thus on photosynthesis and growth.

4.4. Sources of error in stand transpiration estimates

The main sources of error in estimating stand transpiration from sap flux data are due to the radial, azimuthal, and tree-to-tree variation (see e.g. Moon et al., 2015). Two intensive studies on broad leaved trees at our site show that there is a significant decline of 50% in xylem sap flux from a xylem depth of 0–20 mm to a xylem depth of 20–40 mm (Kunert et al., 2015a; Kunert et al., 2013). Conductive xylem depth in those trees was up to 30 mm thus only half of the second profile depth (20–40 mm) was conductive. Xylem sap was flowing along the deeper probe only along half of its length, probably with the same velocity as in the outer xylem, but this still reduced the probe's output by half. This seems to be a general relationship and, hence, a good estimate of the conductive sapwood prevents errors in the upscaling process. Nevertheless, the estimates of the conductive sapwood area contributed with a coefficient of variation of 103.6% as the largest error in estimating stand transpiration rates. Despite the high coefficient of variation of our allometric equation, the uncertainty for the plot level estimates of the conductive sapwood area (A_{plot}) in relative terms was 14.1%. The uncertainty increased with size class and while in the smaller size classes the uncertainty was very low (3.4 and 3.5% for 10–20 cm and 20–30 cm, respectively) it reached a maximum of 7.7% in the large diameter class. This is a common problem of allometric models as they lack in reliable data for the largest diam-

eter classes (Chave et al., 2004) due to a multitude of influences, such as tree age, stand position and density. Azimuthal variation in xylem sap flux is assumed to be related to sun exposure (Shinohara et al., 2013) or asymmetrical crown shapes (Van de Wal et al., 2015). There was no significant variation of xylem sap flux between the two sap flux probes installed per tree at our site. We speculate that this might be due to the almost regular sun exposure with the sun in the zenith throughout the entire year and to constant flat terrain. Trees in our study mostly had symmetrical crown structure.

Tree to tree variation in xylem sap flux in our study was very low and the coefficient of variation among the different size classes was on average 32.3%. Xylem sap flux density has been observed to widely vary among tropical trees and ranging from 5 to 70 g cm^2 h^{-1} (Dierick et al., 2010). However, it has also been reported that xylem sap flux scales with stem diameter in old growth forests (Andrade et al., 2005) and that variation from this relationship might occur only in disturbed stands (Kunert et al., 2015b). Our results show that the variation in maximum whole-tree water use was more pronounced among trees differing in size and crown status than among species (Fig. 5). Those values contain an apparent error due to the high autocorrelation within the conversion process from J_s to Q by using our allometric sap wood equation, but might reflect the upper limit of tree transpiration in wet environments. This has been described before for tropical forests, and justifies the upscaling approach using the diameter-water use relationship (Meinzer et al., 2001; Motzer et al., 2005). Moon et al. (2015) describes the error in the stand transpiration estimates caused by tree to tree variations as minimal in comparison to the error in the estimation of, for example, the conductive sap wood area.

The complex structure of tropical forests, in our case the few large trees occupying the majority of the canopy area and shading many others, might thus explain the higher tree-to-tree variation in xylem sap fluxes compared to temperate or other more seasonal

tropical forest ecosystems (Granier et al., 1996a). Nevertheless, our estimates of stand transpiration are in accord with other studies from the Neotropics. We found that canopy trees transpire $0.09 \, mm \, d^{-1}$ on a very wet and rainy day and up to $5.87 \, mm \, d^{-1}$ on a cloud free and dry day during the driest month of the year. A study from the Guyana with a similar forest formation reports maximum values between 2.3 and $4.5 \, mm \, d^{-1}$ attributing the difference in daily transpiration rates mostly to changes in vapor pressure deficit (Granier et al., 1996b). But very low transpiration rates are also known from other tropical forests. Horna et al. (2011) found only transpiration rates between 0.09 and the maximum $1.05 \, mm \, d^{-1}$ in a perhumid forest in Indonesia, but this can be mostly explained by the on average over 5 times lower xylem sap flux densities compared to our study. Aparecido et al. (2016) report that on average transpiration ranged around $0.3–2.0 \, mm \, day^{-1}$ in wet and dry conditions in a premontane tropical forest in Costa Rica, respectively. But, trees in the understory did not surpass $0.05 \, mm \, day^{-1}$ under any ambient condition, and fluxes from dominant trees did not decrease below $0.5 \, mm \, day^{-1}$ during wet days.

5. Conclusion

We were able to provide further evidence for the three different theories presented. First, the "convergence theory" (Meinzer et al., 2001) resulting in the strong size dependency of tropical tree water use holds for trees in the Central Amazon. Under given environmental conditions, tree size is the most important regulating factor for tree transpiration in tropical old growth forests. Second, we found supporting evidence for the "rainfall recycling theory" by confirming that tropical moist forests actively returns about 37% of the rainfall back to the atmosphere. Third, besides other factors like lower leaf herbivore pressure and the need to sprout new epiphyll-free "clean" leaves, low cloud coverage and higher evaporation demand of the atmosphere might have been the trigger of evolutionary factors for evolving the "greening" in the Amazon during the dry season as those conditions favor high assimilation and transpiration rates. We could further highlight the hydrological importance of large trees in tropical moist forest ecosystems and that they are a very crucial ecological component of tropical forest. Besides storing the largest fraction of stand biomass, large trees are responsible for transpiring large amounts of water back to the atmosphere. Even if large trees take up water from very deep soil layers during dry season and have a very large water storage capacity in their trunks, large trees are also the most vulnerable trees in the forests as they might be the trees most likely to be affected by hydraulic failure under severe water stress situations.

Acknowledgments

References

Andrade, J., Meinzer, F., Goldstein, G., Schnitzer, S., 2005. Water uptake and transport in lianas and co-occurring trees of a seasonally dry tropical forest. Trees 19 (3), 282–289.

Anhuf, D., Motzer, T., Rollenbeck, R., Schröder, B., Szarzynski, J., 1999. Water budget of the Surumoni Crane Site (Venezuela). Selbyana 20 (1), 179–185.

Anon, 1998. How much lumber in that tree? In: office, U.P.F.E. (Ed.), Extension Bulletin. Michigan State University, Michigan.

Aparecido, L.M.T., Miller, G.R., Cahill, A.T., Moore, G.W., 2016. Comparison of tree transpiration under wet and dry canopy conditions in a Costa Rican premontane tropical forest. Hydrol. Processes 30 (26), 5000–5011.

Araújo, A.C., et al., 2002. Comparative measurements of carbon dioxide fluxes from two nearby towers in a central Amazonian rainforest: the Manaus LBA site. J. Geophys. Res.: Atmos. 107 (D20), 20–58 (LBA 58-1-LBA).

Aragao, L.E.O.C., 2012. Environmental science: the rainforest's water pump. Nature 489 (7415), 217–218.

Brienen, R.J.W., et al., 2015. Long-term decline of the Amazon carbon sink. Nature 519 (7543), 344–348.

Brown, I.F., et al., 1995. Uncertainty in the biomass of Amazonian forests: an example from Rondônia, Brazil. For. Ecol. Manage. 75 (1), 175–189.

Chambers, J.Q., Santos, J.d., Ribeiro, R.J., Higuchi, N., 2001. Tree damage, allometric relationships, and above-ground net primary production in central Amazon forest. For. Ecol. Manage. 152 (1–3), 73–84.

Chambers, J.Q., et al., 2004. Respiration from a tropical forest ecosystem: partitioning of sources and low carbon use efficiency. Ecol. Appl. 14 (sp4), 72–88.

Chave, J., et al., 2004. Error propagation and scaling for tropical forest biomass estimates. Philos. Trans. R. Soc. Lond. Ser. B: Biol. Sci. 359 (1443), 409–420.

da Rocha, H.R., et al., 2004. Seasonality of water and heat fluxes over a tropical forest in eastern Amazonia. Ecol. Appl. 14 (sp4), 22–32.

Dünisch, O., Morais, R., 2002. Regulation of xylem sap flow in an evergreen, a semi-deciduous, and a deciduous Meliaceae species from the Amazon. Trees 16 (6), 404–416.

Dierick, D., Hölscher, D., 2009. Species-specific tree water use characteristics in reforestation stands in the Philippines. Agric. For. Meteorol. 149 (8), 1317–1326.

Dierick, D., Kunert, N., Köhler, M., Schwendenmann, L., Hölscher, D., et al., 2010. Comparison of tree water use characteristics in reforestation and agroforestry stands across the tropics. In: Tscharntke, T. (Ed.), Tropical Rainforests and Agroforests Under Global Change. Spinger, Berlin, pp. 293–308.

Dietrich, W., Windsor, M., Dunne, T., 1996. Geology, climate and hydrology of Barro Colorado Island. In: Leigh, J.G.E., Rand, A.S., Windsor, D.M. (Eds.), The Ecology of a Tropical Forest. Seasonal Rhythms and Annual Changes. Smithsonian Institution Press, Washington, DC, pp. 21–46.

Eltahir, E.A.B., Bras, R.L., 1996. Precipitation recycling. Rev. Geophys. 34 (3), 367–378.

Ford, C.R., Hubbard, R.M., Kloeppel, B.D., Vose, J.M., 2007. A comparison of sap flux-based evapotranspiration estimates with catchment-scale water balance. Agric. For. Meteorol. 145 (3–4), 176–185.

Ghazoul, J., Sheil, D., 2010. Tropical Rain Forest Ecology, Diversity, and Conservation. Oxford University Press, Oxford.

Giambelluca, T.W., Ziegler, A.D., Nullet, M.A., Truong, D.M., Tran, L.T., 2003. Transpiration in a small tropical forest patch. Agric. For. Meteorol. 117 (1–2), 1–22.

Granier, A., Biron, P., BrÉ. Da, N., Pontailler, J.Y., Saugier, B., 1996a. Transpiration of trees and forest stands: short and long-term monitoring using sapflow methods. Glob. Change Biol. 2 (3), 265–274.

Granier, A., Huc, R., Barigah, S.T., 1996b. Transpiration of natural rain forest and its dependence on climatic factors. Agric. For. Meteorol. 78 (1–2), 19–29.

Granier, A., Biron, P., Lemoine, D., 2000. Water balance, transpiration and canopy conductance in two beech stands. Agric. For. Meteorol. 100 (4), 291–308.

Granier, A., 1985. Une nouvelle méthode pour la mesure du flux de sève brute dans le tronc des arbres. Ann. For. Sci. 42 (2), 193–200.

Granier, A., 1987. Evaluation of transpiration in a Douglas-fir stand by means of sap flow measurements. Tree Physiol. 3 (4), 309–320.

Higuchi, N., dos Santos, J., Ribeiro, R.J., Minette, Y.B., 1998. Biomassa da parte aérea da vegetação da floresta tropical úmida de terra-firme da Amazônia brasileira. Acta Amazonica 28 (2), 153–166.

Hinckley, T.M., Lassoie, J.P., Running, S.W., 1978. Temporal and spatial variations in the water status of forest trees. For. Sci. 20 (3) (a0001-z0001).

Horna, V., Schuldt, B., Brix, S., Leuschner, C., 2011. Environment and tree size controlling stem sap flux in a perhumid tropical forest of Central Sulawesi. Indonesia. Ann. For. Sci. 68, 1027–1038.

Huete, A.R., et al., 2006. Amazon rainforests green-up with sunlight in dry season. Geophys. Res. Lett. 33 (6).

Jardine, K., et al., 2015. Dimethyl sulfide in the Amazon rain forest. Glob. Biogeochem. Cycles 29 (1), 19–32.

Jung, E.Y., et al., 2011. Up-scaling to stand transpiration of an Asian temperate mixed-deciduous forest from single tree sapflow measurements. Plant Ecol. 212 (3), 383–395.

Katul, G., Kuhn, G., Schieldge, J., Hsieh, C.-I., 1997. The ejection-sweep character of scalar fluxes in the unstable surface layer. Boundary Layer Meteorol. 83 (1), 1–26.

Kleidon, A., Heimann, M., 2000. Assessing the role of deep rooted vegetation in the climate system with model simulations: mechanism, comparison to observations and implications for Amazonian deforestation. Clim. Dyn. 16 (2–3), 183–199.

Kunert, N., Mercado Cardenas, A., 2012. Effects of xylem water transport on CO_2 efflux of woody tissue in a tropical tree, Amazonas State, Brazil. Hoehnea 39 (1), 139–144.

Kunert, N., Schwendenmann, L., Potvin, C., Hölscher, D., 2012. Tree diversity enhances tree transpiration in a Panamanian forest plantation. J. Appl. Ecol. 49 (1), 135–144.

Kunert, N., Barros, P., Higuchi, N., 2013. Do palm water use characteristics explain the spatial distribution of palms in the Central Amazon? Acta Hortic. 991, 197–204.

Kunert, N., Aparecido, L.M.T., Barros, P., Higuchi, N., 2015a. Modeling potential impacts of planting palms or tree in small holder fruit plantations on ecohydrological processes in the central amazon. Forests 6 (8), 2530–2544.

Kunert, N., Aparecido, L.M.T., Higuchi, N., Santos, J.D., Trumbore, S., 2015b. Higher tree transpiration due to road-associated edge effects in a tropical moist lowland forest. Agric. For. Meteorol. 213 (0), 183–192.

Kunert, N., 2016. Curios relationship revealed by looking at long term data sets—the geometry and allometric scaling of diel xylem sap flux in tropical trees. J. Plant Physiol. 205, 80–83.

Leopoldo, P.R., Franken, W.K., Salati, e., 1982. Balanço hídrico de pequena bacia hidrográfica em floresta amazônica de terra firme. Acta Amazonica 12 (2), 33–337.

Lindenmayer, D.B., Laurance, W.F., Franklin, J.F., 2012. Global decline in large old trees. Science 338 (6112), 1305–1306.

Meinzer, F.C., et al., 1997. Control of transpiration from the upper canopy of a tropical forest: the role of stomatal, boundary layer and hydraulic architecture components Plant. Cell Environ. 20 (10), 1242–1252.

Meinzer, F., et al., 1999. Partitioning of soil water among canopy trees in a seasonally dry tropical forest. Oecologia 21, 293–301.

Meinzer, F.C., Goldstein, G., Andrade, J.L., 2001. Regulation of water flux through tropical forest canopy trees: do universal rules apply? Tree Physiol. 21 (1), 19–26.

Meinzer, F.C., James, S.A., Goldstein, G., 2004. Dynamics of transpiration, sap flow and use of stored water in tropical forest canopy trees. Tree Physiol. 24 (8), 901–909.

Moon, M., et al., 2015. Variation in sap flux density and its effect on stand transpiration estimates of Korean pine stands. J. For. Res. 20 (1), 85–93.

Moore, G.W., Bond, B.J., Jones, J.A., Meinzer, F.C., 2010. Thermal-dissipation sap flow sensors may not yield consistent sap-flux estimates over multiple years. Trees 24 (1), 165–174.

Morton, D.C., et al., 2014. Amazon forests maintain consistent canopy structure and greenness during the dry season. Nature 506 (1), 221–224.

Motzer, T., Munz, N., Küppers, M., Schmitt, D., Anhuf, D., 2005. Stomatal conductance, transpiration and sap flow of tropical montane rain forest trees in the southern Ecuadorian Andes. Tree Physiol. 25 (10), 1283–1293.

Nakai, T., Shimoyama, K., 2012. Ultrasonic anemometer angle of attack errors under turbulent conditions. Agric. For. Meteorol. 162–163, 14–26.

Nepstad, D.C., et al., 1994. The role of deep roots in the hydrological and carbon cycles of Amazonian forests and pastures. Nature 372 (6507), 666–669.

O'Brien, J.J., Oberbauer, S.F., Clark, D.B., 2004. Whole tree xylem sap flow responses to multiple environmental variables in a wet tropical forest Plant. Cell Environ. 27 (5), 551–567.

Parolin, P., Müller, E., Junk, W., 2008. Sapwood area in seven common tree species of Central Amazon floodplains. Area Pesquisas Bot. 59, 277–286.

Salati, E., Vose, P.B., 1984. Amazon basin: a system in equilibrium. Science 225 (4658), 129–138.

Saleska, S.R., et al., 2003. Carbon in amazon forests: unexpected seasonal fluxes and disturbance-induced losses. Science 302 (5650), 1554–1557.

Schneebeli, M., Wolf, S., Kunert, N., Eugster, W., Mätzler, C., 2011. Relating the X-band opacity of a tropical tree canopy to sapflow, rain interception and dew formation. Remote Sens. Environ. 115 (8), 2116–2125.

Schwendenmann, L., Pendall, E., Sanchez-Bragado, R., Kunert, N., Hölscher, D., 2015. Tree water uptake in a tropical plantation varying in tree diversity: interspecific differences, seasonal shifts and complementarity. Ecohydrology 8 (1), 1–12.

Shinohara, Y., et al., 2013. Azimuthal and radial variations in sap flux density and effects on stand-scale transpiration estimates in a Japanese cedar forest. Tree Physiol. 33 (5), 550–558.

Shuttleworth, W.J., et al., 1984. Eddy correlation measurements of energy partition for Amazonian forest. Q. J. R. Meteorol. Soc. 110 (466), 1143–1162.

Slik, J.W.F., et al., 2013. Large trees drive forest aboveground biomass variation in moist lowland forests across the tropics. Glob. Ecol. Biogeogr. 22 (12), 1261–1271.

Spracklen, D.V., Arnold, S.R., Taylor, C.M., 2012. Observations of increased tropical rainfall preceded by air passage over forests. Nature 489 (7415), 282–285.

Tyree, M.T., Ewers, F.W., 1996. Hydraulic architecture of woody tropical plants. In: Mulkey, S.S., Chazdon, R.L., Smith, A.P. (Eds.), Tropical Forest Plant Ecophysiology. Chapman and Hall, New York, pp. 217–243.

ter Steege, H., et al., 2013. Hyperdominance in the amazonian tree flora. Science 342 (6156).

Van de Wal, B.A.E., Guyot, A., Lovelock, C.E., Lockington, D.A., Steppe, K., 2015. Influence of temporospatial variation in sap flux density on estimates of whole-tree water use in Avicennia marina. Trees 29 (1), 215–222.

Vieira, S., et al., 2004. Forest structure and carbon dynamics in amazonian tropical rain forests. Oecologia 140 (3), 468–479.

Villa Nova, N.A., Salati, E., Matsui, E., 1976. Estimativa de evapotranspiração na Bacia Amazônica. Acta Amazonica 6 (2), 215–228.

Wohl, E.E., 2007. Hydrology and discharge. In: Gupta, A. (Ed.), Large Rivers: Geomorphology and Management. John Wiley & Sons, UK, pp. 29–40.

Wright, S.J., Schaik, C.P.V., 1994. Light and the phenology of tropical trees. Am. Naturalist 143 (1), 192–199.

Yepez, E.A., Williams, D.G., Scott, R.L., Lin, G., 2003. Partitioning overstory and understory evapotranspiration in a semiarid savanna woodland from the isotopic composition of water vapor. Agric. Forest Meteorol. 119 (1–2), 53–68.